FUDMA Journal of Sciences (FJS)
ISSN online: 2616-1370
ISSN print: 2645 - 2944
Vol. 7 No. 4, August, 2023, pp 357 - 368
DOI: https://doi.org/10.33003/fjs-2023-0704-1933

APPLICATION OF NON-STANDARD FINITE DIFFERENCE METHOD ON COVID-19 MATHEMATICAL MODEL WITH FEAR OF INFECTION

[1]Usman, I. G., [2]Ibrahim, M. O., [3]Isah, B. Y., [4]Lawal, N., *[5]Akinyemi, S. T.

[1]Department of Mathematics, Zamfara State College of Education, Maru, Nigeria
[2]Department of Mathematics, University of Ilorin, Kwara State, Nigeria
[3]Department of Mathematics, Usmanu Danfodio University, Sokoto State, Nigeria
[4]Department of Veterinary Microbiology, Usmanu Danfodio University, Sokoto State, Nigeria
[5]Department of Mathematics, Sikiru Adetona College of Education, Science and Technology, Ogun State, Nigeria

*Corresponding authors' email: sammysalt047@gmail.com

ABSTRACT

This study presents a novel application of Non -Standard Finite Difference (NSFD) Method to solve a COVID-19 epidemic mathematical model with the impact of fear due to infection. The mathematical model is governed by a system of first-order non-linear ordinary differential equations and is shown to possess a unique positive solution that is bounded. The proposed numerical scheme is used to obtain an approximate solution for the COVID-19 model. Graphical results were displayed to show that the solution obtained by NSFD agrees well with those obtained by the Runge-Kutta-Fehlberg method built-in Maple 18.

Keywords: Differential Equations, COVID-19 Mathematical Model, Non-Standard Finite Difference, Approximate Solution

INTRODUCTION

The use of differential equations to model the transmission dynamics of infectious disease can be traced back to 1970 when Daniel Bernoulli justified the use of inoculation to curb the spread of smallpox (Dietz and Heesterbeek, 2002; Foppa, 2017). These models are usually nonlinear (Peter et al., 2020; Gu et al., 2023; Akinyemi et al., 2023; Kambali et al., 2023; Ochi et al., 2023) and are difficult to obtain their exact solution (Onwubuoya et al., 2018b; Riyapan et al., 2021; ur Rehman et al., 2023).

Thus, numerical methods are used to obtain approximate solutions. Some of the numerical techniques are Euler (Ashigi et al., 2021; Mohammed et al., 2021; Reza et al., 2022), Euler Predictor Corrector (Onwubuoya et al., 2018a), Non-Standard Finite Difference (Raza et al., 2022; Butt et al., 2023; ur Rehman et al., 2023).

The Non-Standard Finite Difference (NSFD) method developed by Ronald E. Mickens is a discrete representation of a continuous model (Mickens and Washington, 2012, Qui et al., 2014). Apart from predicting the behaviour of the dynamical system correctly, the NSFD method is known to preserve the dynamical properties of an epidemic model and is less difficult to implement when compared with the aforementioned numerical methods (Qui et al., 2014). Applications of NSFD method are found in financial theory (Mehdizadeh et al., 2022; Mehdizadeh et al., 2023), epidemiology (ur Rehman et al., 2023, Butt et al., 2023), enzymology (Miller & O'Riordan, 2020; Zafar et al., 2023), pharmacology (Egbelowo, 2018; Ebgelowo & Hoang, 2021), immunology (Costa et al., 2023; Elaiw et al., 2023).

The purpose of this study is to apply the NSFD scheme to solve a mathematical model presented in Ibrahim (2023). The mathematical model proposed by Ibrahim (2023), describes the spread of COVID-19 in the presence of fear of infection and is governed by the following system of nonlinear differential equations.

$$\left.\begin{aligned}
\frac{dS}{dt} &= P - \Omega S - K_1 S + \nu_2 V\\
\frac{dV}{dt} &= \nu_1 S - e\Omega V - K_2 V\\
\frac{dE}{dt} &= \Omega(S + eV) - K_3 E\\
\frac{dQ}{dt} &= \tau_1 E - K_4 Q\\
\frac{dA}{dt} &= \theta_1 E - K_5 A\\
\frac{dI}{dt} &= \theta_2 A - K_6 I\\
\frac{dH}{dt} &= \theta_3 Q + \tau_2 I - K_7 H\\
\frac{dR}{dt} &= \alpha_1 A + \alpha_2 I + \alpha_3 H - \mu R\\
\frac{dD}{dt} &= l_1 A + l_2 I + l_3 H - \phi D\\
\frac{dW}{dt} &= \Pi I + \Pi \vartheta H - \varepsilon W
\end{aligned}\right\} \quad (1)$$

Subject to $S(0) = 1.885103470 \times 10^8$, $V(0) = 2.672 \times 10^7$, $E(0) = 3{,}500$, $Q(0) = 400$, $A(0) = 1{,}247$, $I(0) = 800$, $H(0) = 652$, $R(0) = 249{,}911$, $D(0) = 3143$ and $W(0) = 1000$.

$$\Omega = \frac{\beta(A\eta_1 + H\eta_2 + W\eta_3 + I)}{\chi_1 D + 1},\ K_1 = \mu + \nu_1,\ K_2 = \mu + \nu_2,\ K_3 = \mu + \theta_1 + \tau_1,\ K_4 = \mu + \theta_3,\ K_5 = \mu + \theta_2 + \alpha_1 + \delta_1,$$

$K_6 = \mu + \tau_2 + \alpha_2 + \delta_2$, $K_7 = \mu + \alpha_3 + \delta_3$, $l_1 = \mu + \delta_1$, $l_2 = \mu + \delta_2$, $l_3 = \mu + \delta_3$ and $e = 1 - b$.

Table 1: Description of State Variables of the Model

State Variable	Meaning
$S(t)$	Unvaccinated Susceptible Individuals
$V(t)$	Vaccinated Susceptible Individuals
$E(t)$	Exposed Individuals
$Q(t)$	Quarantined Individuals

$A(t)$	Asymptomatic Individuals
$I(t)$	Symptomatic Individuals
$H(t)$	Hospitalized Individuals
$R(t)$	Recovered Individuals
$D(t)$	COVID-19 Dead Individuals
$W(t)$	Concentration of COVID-19 Viruses in the Environment

Table 2: Description of Parameters for the Model

Parameters	Description of Parameters	Hypothetical Values	Source
N_0	Total Population of Active Humans	215,497,404	Worldometer, 2022
P	Recruitment rate.	$\boldsymbol{\mu N_0}$	Estimated
μ_0	Estimated average life span of Nigerian	55.75 per year	Worldometer, 2022
μ	Natural death rate.	$\frac{1}{\mu_0 \times 365}$per day	Estimated
δ_1, δ_2, δ_3	COVID-19 induced death rate for individuals in A, I and H compartments respectively.	0.018, 0.025, 0.01	Estimated Nana-Kyere et al., 2022
α_1, c α_3	The recovery rate for individuals in A, I and Hcompartments respectively.	0.0195692, 0.004165, 0.0701	Diagne et al., 2021
b	Rate of COVID-19 efficacy	0.6309	WHO, 2021
v_1	Vaccination rate for susceptible individuals	0.4	Diagne et al., 2021
v_2	Waning rate of COVID-19 vaccine	0.095	Paul and Kuddus, 2022
τ_1	Quarantine rate for exposed individuals	0.012	Nana-Kyere et al., 2022
θ_1, θ_2	Progression rate for individuals in E to A and A to I compartments respectively	0.7,0.08	Srivastav et al., 2021
θ_3, τ_2	The hospitalization rate for individuals in Q and I compartments respectively.	0.06, 0.02	Nana-Kyere et al., 2022
η_1, η_2, η_3	Modification parameters associated with reduction of infectiousness for individuals in A, H and W as compared to I class respectively.	0.75, 0.5, 0.33	Garba et al., 2020
π	Shedding rate of coronavirus into the environment.	0.002	Garba et al., 2020
ϑ	Modification parameters associated with reduction of shedding for individuals in H as compared to I class respectively.	0.5	Garba et al., 2020
ε	The decay rate of coronavirus in the environment.	0.85	Garba et al., 2020
ϕ	Burial rate of dead infectious individuals.	0.2276	Aba Oud et al., 2021
χ_1	Level of fear associated with COVID-19 infection.	(0,1)	Estimated
$\boldsymbol{\beta}$	COVID-19 transmission coefficient	$\frac{\beta_0}{N_0}$ $\beta_0 = 0.1086$	Estimated Adewole et al., 2021

The rest of this paper is arranged as follows: Section 2 presents the material and methods. Results and discussion are addressed in Section 3. Section 4 gives the conclusion of the study.

MATERIALS AND METHODS

This section deals with the introduction to NSFD, the dynamical properties of Model (1) and the application of NSFD on Model (1).

Basic Concept of NSFD

First, we consider an autonomous ordinary differential equation of the form

$$\frac{dx}{dt} = f\big(x(t)\big) \tag{2}$$

Definition 1: A discretized form of (2) is called an NSFD scheme provided at least one of these conditions is satisfied.

1. The discretized representation of (2) is

$$\frac{dx}{dt} \to \frac{x_{n+1} - G(h)x_n}{Z(h)} \qquad n = 0,1,\cdots M-1 \tag{3}$$

such that $t_n = t_0 + hn,\ x_n = x(t_n),\ h = \frac{T}{M}$ the numerator function $G(h) = 1 + O(h)$, and the denominator function $Z(h) = h + O\big(h^2\big)$.

2. The nonlinear term $f(x)$ in (2) should be approximated using the nonlocal discretized form. For instance,

$$x^2 \approx x_n x_{n+1} \tag{4}$$

Here, T is the final time, h the time step size and M the number of iterations. Again, we consider a system of first-order nonlinear differential equations

$$\left.\begin{aligned} \frac{dx_1}{dt} &= -a_1x_1x_2 - b_1x_1 \\ \frac{dx_2}{dt} &= a_1x_1x_2 + b_2x_2 \end{aligned}\right\} \tag{5}$$

subject to $x_1(0) = c_1$ and $x_2(0) = c_2$.

Discretized (5) using the semi-implicit finite scheme while ensuring that the above condition conditions are met to have

$$\left.\begin{aligned} \frac{X_{1,n+1} - G_1X_{1,n}}{Z_1} &= -a_1X_{1,n+1}X_{2,n} - b_1X_{1,n+1} \\ \frac{X_{2,n+1} - G_2X_{2,n}}{Z_2} &= a_1X_{1,n+1}X_{2,n} - b_2X_{2,n+1} \end{aligned}\right\}$$
$$n = 0,1,\cdots M \tag{6}$$

Following Ahmed (2011) and Sweilam et al. (2017), to have $G_1 = G_2 = 1$ and an exponential denominator function $Z_1 = \frac{e^{b_1h}-1}{b_1}$ and $Z_2 = \frac{e^{b_2h}-1}{b_2}$, are used. Hence, (6) becomes

$$\left.\begin{aligned} X_{1,n+1} &= \frac{X_{1,n}}{Z_1(a_1X_{2,n}+b_1)+1} \\ X_{2,n+1} &= \frac{X_{2,n}\big(a_1X_{1,n+1}Z_2+1\big)}{Z_2b_2+1} \end{aligned}\right\} \tag{7}$$

Remark [Sweilam et al. (2017)] : Whenever the denominator function $Z(h) = h$, the scheme is called NSFD-I, otherwise it is called NSFD-II.

Thus, this study utilizes the NSFD-II scheme. Next, the dynamical properties such as the existence and uniqueness, positivity and boundedness solution of Model (1) are examined.

Existence and Uniqueness Solution of the Covid-19 Model

Theorem 2.1: The system (1) has a unique solution in the region $(S,\ V,\ E,\ Q,\ A,\ I,\ H,\ R,\ D,\ W) \in \mathbb{R}_+^{10}$

Proof: We write the right-hand side of Model (1) as

$$\left.\begin{aligned} f_1 &= P - \Omega S - K_1S + \nu_2V \\ f_2 &= \nu_1S - e\Omega V - K_2V \\ f_3 &= \Omega(S + eV) - K_3E \\ f_4 &= \tau_1E - K_4Q \\ f_5 &= \theta_1E - K_5A \\ f_6 &= \theta_2A - K_6I \\ f_7 &= \theta_3Q + \tau_2I - K_7H \\ f_8 &= \alpha_1A + \alpha_2I + \alpha_3H - \mu R \\ f_9 &= l_1A + l_2I + l_3H - \phi D \\ f_{10} &= \Pi I + \Pi\vartheta H - \varepsilon W \end{aligned}\right\} \tag{8}$$

Then the following are obtained

$$\left|\frac{\partial f_1}{\partial S}\right| = |-\Omega - K_1| \le \infty,\ \left|\frac{\partial f_1}{\partial V}\right| = |-\nu_2| \le \infty,\ \left|\frac{\partial f_1}{\partial A}\right| = \left|-\frac{\beta\eta_1S}{\chi_1D+1}\right| \le \infty,\ \left|\frac{\partial f_1}{\partial H}\right| = \left|-\frac{\beta\eta_2S}{\chi_1D+1}\right| \le \infty,\ \left|\frac{\partial f_1}{\partial W}\right| = \left|-\frac{\beta\eta_3S}{\chi_1D+1}\right| \le \infty,\ \left|\frac{\partial f_1}{\partial I}\right| = \left|-\frac{\beta S}{\chi_1D+1}\right| \le \infty,\ \left|\frac{\partial f_1}{\partial E}\right| = \left|\frac{\partial f_1}{\partial Q}\right| = \left|\frac{\partial f_1}{\partial R}\right| = \left|\frac{\partial f_1}{\partial D}\right| = \le 0,$$

$$\left|\frac{\partial f_2}{\partial S}\right| = |\nu_1| \le \infty,\ \left|\frac{\partial f_2}{\partial V}\right| = |-e\Omega - K_2| \le \infty,\ \left|\frac{\partial f_2}{\partial A}\right| = \left|-\frac{\beta\eta_1eV}{\chi_1D+1}\right| \le \infty,\ \left|\frac{\partial f_2}{\partial H}\right| = \left|-\frac{\beta\eta_2eV}{\chi_1D+1}\right| \le \infty,\ \left|\frac{\partial f_2}{\partial W}\right| = \left|-\frac{\beta\eta_3eV}{\chi_1D+1}\right| \le \infty,\ \left|\frac{\partial f_2}{\partial I}\right| = \left|-\frac{\beta eV}{\chi_1D+1}\right| \le \infty,\ \left|\frac{\partial f_2}{\partial E}\right| = \left|\frac{\partial f_2}{\partial Q}\right| = \left|\frac{\partial f_2}{\partial R}\right| = \left|\frac{\partial f_2}{\partial D}\right| = 0 \le \infty,$$

$$\left|\frac{\partial f_3}{\partial S}\right| = |\Omega| \le \infty,\ \left|\frac{\partial f_3}{\partial V}\right| = |e\Omega| \le \infty,\ \left|\frac{\partial f_3}{\partial A}\right| = \left|\frac{\beta\eta_1(S+eV)}{\chi_1D+1}\right| \le \infty,\ \left|\frac{\partial f_3}{\partial H}\right| = \left|\frac{\beta\eta_2(S+eV)}{\chi_1D+1}\right| \le \infty,\ \left|\frac{\partial f_3}{\partial W}\right| = \left|\frac{\beta\eta_3(S+eV)}{\chi_1D+1}\right| \le \infty,\ \left|\frac{\partial f_3}{\partial I}\right| = \left|-\frac{\beta(S+eV)}{\chi_1D+1}\right| \le \infty,\ \left|\frac{\partial f_3}{\partial E}\right| = |-K_3| \le \infty,\ \left|\frac{\partial f_3}{\partial Q}\right| = \left|\frac{\partial f_3}{\partial R}\right| = \left|\frac{\partial f_3}{\partial D}\right| = 0 \le \infty,$$

$$\left|\frac{\partial f_4}{\partial S}\right| = \left|\frac{\partial f_4}{\partial V}\right| = \left|\frac{\partial f_4}{\partial A}\right| = \left|\frac{\partial f_4}{\partial I}\right| = \left|\frac{\partial f_4}{\partial H}\right| = \left|\frac{\partial f_4}{\partial R}\right| = \left|\frac{\partial f_4}{\partial D}\right| = \left|\frac{\partial f_4}{\partial W}\right| = 0 \le \infty,\ \left|\frac{\partial f_4}{\partial E}\right| = |\tau_1| \le \infty,\ \left|\frac{\partial f_4}{\partial Q}\right| = |-K_4| \le \infty,$$

$$\left|\frac{\partial f_5}{\partial S}\right| = \left|\frac{\partial f_5}{\partial V}\right| = \left|\frac{\partial f_5}{\partial Q}\right| = \left|\frac{\partial f_5}{\partial I}\right| = \left|\frac{\partial f_5}{\partial H}\right| = \left|\frac{\partial f_5}{\partial R}\right| = \left|\frac{\partial f_5}{\partial D}\right| = \left|\frac{\partial f_5}{\partial W}\right| = 0 \le \infty,\ \left|\frac{\partial f_5}{\partial E}\right| = |\theta_1| \le \infty,\ \left|\frac{\partial f_5}{\partial A}\right| = |-K_5| \le \infty,$$

$$\left|\frac{\partial f_6}{\partial S}\right| = \left|\frac{\partial f_6}{\partial V}\right| = \left|\frac{\partial f_6}{\partial E}\right| = \left|\frac{\partial f_6}{\partial Q}\right| = \left|\frac{\partial f_6}{\partial H}\right| = \left|\frac{\partial f_6}{\partial R}\right| = \left|\frac{\partial f_6}{\partial D}\right| = \left|\frac{\partial f_6}{\partial W}\right| = 0 \le \infty,\ \left|\frac{\partial f_6}{\partial A}\right| = |\theta_1| \le \infty,\ \left|\frac{\partial f_6}{\partial I}\right| = |-K_6| \le \infty,$$

$$\left|\frac{\partial f_7}{\partial S}\right| = \left|\frac{\partial f_7}{\partial V}\right| = \left|\frac{\partial f_7}{\partial E}\right| = \left|\frac{\partial f_7}{\partial A}\right| = \left|\frac{\partial f_7}{\partial R}\right| = \left|\frac{\partial f_7}{\partial D}\right| = \left|\frac{\partial f_7}{\partial W}\right| = 0 \le \infty,\ \left|\frac{\partial f_7}{\partial Q}\right| = |\theta_3| \le \infty\ \left|\frac{\partial f_7}{\partial I}\right| = |\tau_2| \le \infty,\ \left|\frac{\partial f_7}{\partial H}\right| = |-K_7| \le \infty,$$

$$\left|\frac{\partial f_8}{\partial S}\right| = \left|\frac{\partial f_8}{\partial V}\right| = \left|\frac{\partial f_8}{\partial E}\right| = \left|\frac{\partial f_8}{\partial Q}\right| = \left|\frac{\partial f_8}{\partial D}\right| = \left|\frac{\partial f_8}{\partial W}\right| = 0 \le \infty,\ \left|\frac{\partial f_8}{\partial A}\right| = |\alpha_1| \le \infty\ \left|\frac{\partial f_8}{\partial I}\right| = |\alpha_2| \le \infty,\ \left|\frac{\partial f_8}{\partial H}\right| = |\alpha_3| \le \infty.\ \left|\frac{\partial f_8}{\partial R}\right| = |-\mu| \le \infty,$$

$$\left|\frac{\partial f_9}{\partial S}\right| = \left|\frac{\partial f_9}{\partial V}\right| = \left|\frac{\partial f_9}{\partial E}\right| = \left|\frac{\partial f_9}{\partial Q}\right| = \left|\frac{\partial f_9}{\partial R}\right| = \left|\frac{\partial f_9}{\partial W}\right| = 0 \le \infty,\ \left|\frac{\partial f_9}{\partial A}\right| = |l_1| \le \infty\ \left|\frac{\partial f_9}{\partial I}\right| = |l_2| \le \infty,\ \left|\frac{\partial f_9}{\partial H}\right| = |l_3| \le \infty,\ \left|\frac{\partial f_9}{\partial D}\right| = |-\phi| \le \infty,$$

$$\left|\frac{\partial f_8}{\partial S}\right| = \left|\frac{\partial f_{10}}{\partial V}\right| = \left|\frac{\partial f_{10}}{\partial E}\right| = \left|\frac{\partial f_{10}}{\partial A}\right| = \left|\frac{\partial f_{10}}{\partial Q}\right| = \left|\frac{\partial f_{10}}{\partial D}\right| = \left|\frac{\partial f_{10}}{\partial R}\right| = 0 \le \infty,\ \left|\frac{\partial f_{10}}{\partial I}\right| = |\Pi| \le \infty,\ \left|\frac{\partial f_{10}}{\partial H}\right| = |\Pi\vartheta| \le \infty, \text{ and } \left|\frac{\partial f_{10}}{\partial W}\right| = |-\varepsilon| \le \infty.$$

Since, all the partial derivatives are continuous and bounded, then by Derrick and Grossman's theorem in Derrick and Grossman (1987) and Rabiu and Akinyemi (2016), the unique solution of Model (1) is established.

Positivity Solution of the Covid-19 Model

Theorem 2.2: The solution set $\{S(t), V(t), E(t), Q(t), A(t), I(t), H(t), R(t), D(t), W(t)\}$ of Model (1) is non-negative $\forall t \ge 0$, provided the initial conditions are non-negative.

Proof: It is readily seen that the first equation of Model (1) satisfies

$$\frac{dS}{dt} \ge -(\Omega + K_1)S \tag{9}$$

Solve (9) using the separable variable techniques to obtain

$$S(t) \ge S(0)e^{-\left(\int_0^t \Omega(q)dq + K_1 t\right)} \ge 0 \qquad \forall t \ge 0.$$

Similarly, the second equation of system (1) gives

$$\frac{dV}{dt} \ge -(e\Omega + K_2)V \tag{10}$$

The solution of (10) gives

$$V(t) \ge V(0)e^{-\left(\int_0^t e\Omega(q)dq + K_2 t\right)} \ge 0 \qquad \forall t \ge 0.$$

Following a similar argument, the rest equations of system (1) yields

$$\left.\begin{aligned}
&E(t) \ge E(0)e^{-K_3 t} \ge 0 \qquad \forall t \ge 0,\\
&Q(t) \ge Q(0)e^{-K_4 t} \ge 0 \qquad \forall t \ge 0,\\
&A(t) \ge A(0)e^{-K_5 t} \ge 0 \qquad \forall t \ge 0,\\
&I(t) \ge I(0)e^{-K_6 t} \ge 0 \qquad \forall t \ge 0,\\
&H(t) \ge H(0)e^{-K_7 t} \ge 0 \qquad \forall t \ge 0,\\
&R(t) \ge R(0)e^{-\mu t} \ge 0 \qquad \forall t \ge 0,\\
&D(t) \ge D(0)e^{-\phi t} \ge 0 \qquad \forall t \ge 0,\\
&W(t) \ge W(0)e^{-\varepsilon t} \ge 0 \qquad \forall t \ge 0.
\end{aligned}\right\} \tag{11}$$

Hence, the state variables are non-negative since their initial conditions $\big(S(0),\ V(0),\ E(0),\ Q(0),\ A(0),\ I(0),\ H(0),\ R(0),\ D(0),\ W(0)\big)$ are not negative. Hence, we conclude the proof.

Boundedness of Solution

Theorem 3: The set $\Theta = \left\{(S, V, E, Q, A, I, H, R, D, W) \in \mathbb{R}_+^{10}:\ N \le \frac{P}{\mu};\ D \le \frac{d_1 P}{\phi\mu};\ W \le \frac{P\Pi(1+\vartheta)}{\mu\varepsilon}\right\}$ is positively invariant and attractive with respect to Model (1)

Proof: Since $N(t) = S(t) + V(t) + E(t) + Q(t) + I(t) + H(t) + R(t)$ then the rate of change of the total active population has been obtained by adding the first-eighth equations of the system (1) to get

$$\frac{dN}{dt} = P - \mu N - \delta_1 A - \delta_2 I - \delta_3 H \tag{12}$$

It is readily seen that (12) becomes

$$\frac{dN}{dt} \le P - \mu N \tag{13}$$

Solve (13) by integrating factor to have

$$N(t) \le \frac{P}{\mu} + \left(N(0) - \frac{P}{\mu}\right)e^{-\mu t} \qquad \forall t \ge 0. \tag{14}$$

Therefore as $t \to \infty,\ 0 \le N(t) \le \frac{P}{\mu}$.

It is readily seen that $A(t) \le \frac{P}{\mu},\ I(t) \le \frac{P}{\mu}$, and $H(t) \le \frac{P}{\mu}$, since $0 \le N(t) \le \frac{P}{\mu}$. Then. The ninth equation of the system (1) gives

$$\frac{dD}{dt} \le \frac{d_1 P}{\mu} - \phi D \tag{15}$$

Where $d_1 = \delta_1 + \delta_2 + \delta_3 + 3\mu$

The solution of (15) yields

$$D(t) \le \frac{d_1 P}{\phi\mu} + \left(D(0) - \frac{d_1 P}{\phi\mu}\right)e^{-\phi t} \qquad \forall t \ge 0. \tag{16}$$

As $t \to \infty,\ 0 \le D(t) \le \frac{d_1 P}{\phi\mu}$.
Similarly, the solution of the last equation of system (1) is obtained as

$$W(t)\ \le \frac{P\Pi(1+\vartheta)}{\mu\varepsilon} + \left(W(0) - \frac{P\Pi(1+\vartheta)}{\mu\varepsilon}\right)e^{-\varepsilon t} \qquad \forall t \ge 0. \tag{17}$$

Hence, as $t \to \infty,\ 0 \le W(t)\ \le \frac{P\Pi(1+\vartheta)}{\mu\varepsilon}$. Therefore,$\Theta$ is positively invariant since $N,\ D$ and W are bounded.

Application of NSFD2
The continuous dynamical model (1) is converted to its discrete form based on the rules and steps outlined in Section 2. Thus (1) becomes

$$\frac{S_{n+1}-S_n}{Z_1} = \frac{-\beta(A_n\eta_1+H_n\eta_2+W_n\eta_3+I_n)S_{n+1}}{\chi_1 D_n+1} - K_1 S_{n+1} + V_n\nu_2 + P \tag{18}$$

$$\frac{V_{n+1}-V_n}{Z_2} = \frac{-\beta e(A_n\eta_1+H_n\eta_2+W_n\eta_3+I_n)V_{n+1}}{\chi_1 D_n+1} - K_2 V_{n+1} + S_{n+1}\nu_1 \tag{19}$$

$$\frac{E_{n+1}-E_n}{Z_3} = \frac{-\beta(S_{n+1}+eV_{n+1})(A_n\eta_1+H_n\eta_2+W_n\eta_3+I_n)}{\chi_1 D_n+1} - K_3 E_{n+1} \tag{20}$$

$$\frac{Q_{n+1}-Q_n}{Z_4} = \tau_1 E_{n+1} - K_4 Q_{n+1} \tag{21}$$

$$\frac{A_{n+1}-A_n}{Z_5} = \theta_1 E_{n+1} - K_5 A_{n+1} \tag{22}$$

$$\frac{I_{n+1}-1_n}{Z_6} = \theta_2 A_{n+1} - K_6 I_{n+1} \tag{23}$$

$$\frac{H_{n+1}-H_n}{Z_7} = \theta_3 Q_{n+1} + \tau_2 I_{n+1} - K_7 H_{n+1} \tag{24}$$

$$\frac{R_{n+1}-R_n}{Z_8} = \alpha_1 A_{n+1} + \alpha_2 I_{n+1} + \alpha_3 H_{n+1} - \mu R_{n+1} \tag{25}$$

$$\frac{D_{n+1}-D_n}{Z_9} = l_1 A_{n+1} + l_2 I_{n+1} + l_3 H_{n+1} - \phi D_{n+1} \tag{26}$$

$$\frac{W_{n+1}-W_n}{Z_{10}} = \Pi I_{n+1} + \Pi\vartheta H_{n+1} - \varepsilon W_{n+1} \tag{27}$$

Where,

$$Z_8 = \frac{e^{\mu h}-1}{\mu},\quad Z_9 = \frac{e^{\phi h}-1}{\phi},\quad Z_{10} = \frac{e^{\varepsilon h}-1}{\varepsilon},\ \ and\ Z_i = \frac{e^{K_i h}-1}{K_i} \quad \forall i = 1,\cdots,7. \tag{28}$$

Make $S_{n+1}, V_{n+1}, E_{n+1}, Q_{n+1}, A_{n+1}, I_{n+1}, H_{n+1}, R_{n+1}, D_{n+1}$,and$W_{n+1}$ subject formula from (18)-(27) respectively to have

$$S_{n+1} = \frac{\left((V_n\nu_2+P)Z_1+S_n\right)(\chi_1 D_n+1)}{\left(\Psi_n+(\chi_1 D_n+1)\right)Z_1+\chi_1 D_n+1} \tag{29}$$

$$V_{n+1} = \frac{(S_{n+1}Z_2\nu_2+V_n)(\chi_1 D_n+1)}{\left(e\Psi_n+K_2(\chi_1 D_n+1)\right)Z_2+\chi_1 D_n+1} \tag{30}$$

$$E_{n+1} = \frac{\Psi_n(S_{n+1}+eV_{n+1})Z_3+E_n(\chi_1 D_n+1)}{(K_3 Z_3+1)(\chi_1 D_n+1)} \tag{31}$$

$$Q_{n+1} = \frac{Q_n+E_{n+1}Z_4\tau_1}{K_4 Z_4+1} \tag{32}$$

$$A_{n+1} = \frac{A_n+E_{n+1}Z_5\theta_1}{K_5 Z_5+1} \tag{33}$$

$$I_{n+1} = \frac{I_n+A_{n+1}Z_6\theta_2}{K_6 Z_6+1} \tag{34}$$

$$H_{n+1} = \frac{H_n+I_{n+1}Z_7\tau_2+Q_{n+1}Z_7\theta_3}{K_7 Z_7+1} \tag{35}$$

$$R_{n+1} = \frac{R_n+A_{n+1}Z_8\alpha_1+I_{n+1}Z_8\alpha_2+H_{n+1}Z_8\alpha_2}{\mu Z_8+1} \tag{36}$$

$$D_{n+1} = \frac{D_n+A_{n+1}Z_9 l_1+I_{n+1}Z_9 l_2+H_{n+1}Z_9 l_3}{\phi Z_9+1} \tag{37}$$

$$W_{n+1} = \frac{W_n+I_{n+1}Z_{10}\Pi+H_{n+1}Z_{10}\Pi\vartheta}{\varepsilon Z_{10}+1} \tag{38}$$

Where

$$\Psi_n = \beta(A_n\eta_1+H_n\eta_2+W_n\eta_3+I_n)$$

RESULTS AND DISCUSSION

We simulated the COVID-19 model (29)-(38) for $T = 150$ days while using the initial conditions mentioned above by setting the stepsize $h = 0.01$ for NSFD-II. To validate the reliability of NSFD-II, the result obtained by NSFD-II was compared with the Runge-Kutta-Fehlberg (RKF45) method built-in Maple 18 software.

The results generated by NSFD-II and RKF45 methods for the population of susceptible individuals are displayed in Figure 1. Both methods show a gradual decrease in the population of susceptible humans for about 10 days and become steady for the remaining simulation period.

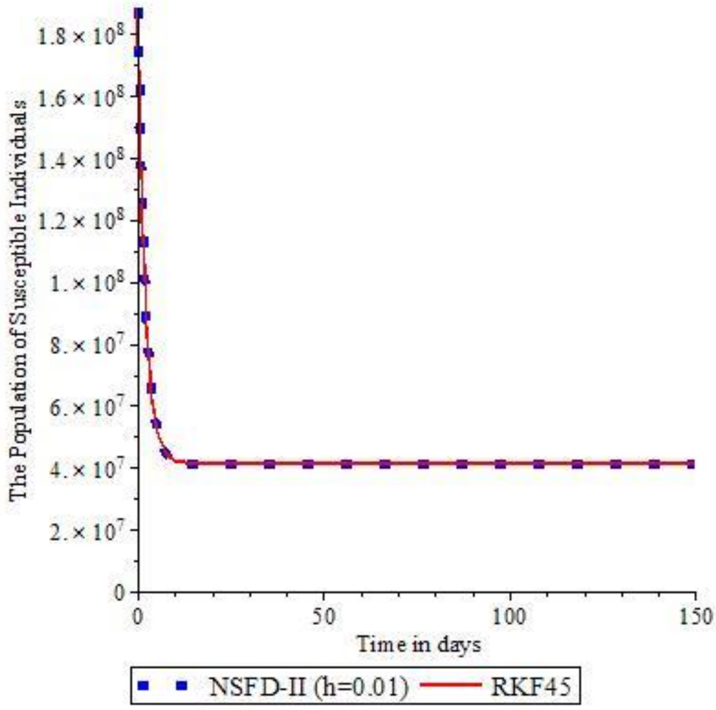

Figure 1: Graphical Comparison for $S(t)$

The population profile for the vaccinated humans obtained by NSFD-II and RKF45 methods is shown in Figure 2. The figure also shows that both methods agree that the population of vaccinated humans gradually increases first, before becoming steady.

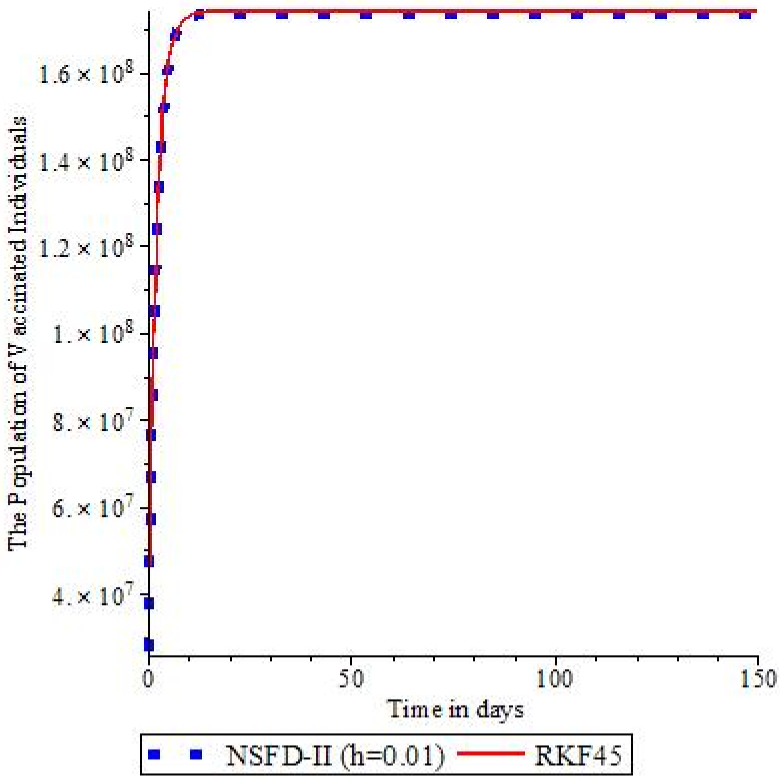

Figure 2: Graphical Comparison for $V(t)$

Figures 3-4 depict the population profile for the exposed and quarantined humans respectively. The figures show that both methods describe that the population of the exposed and quarantined decreases to zero.

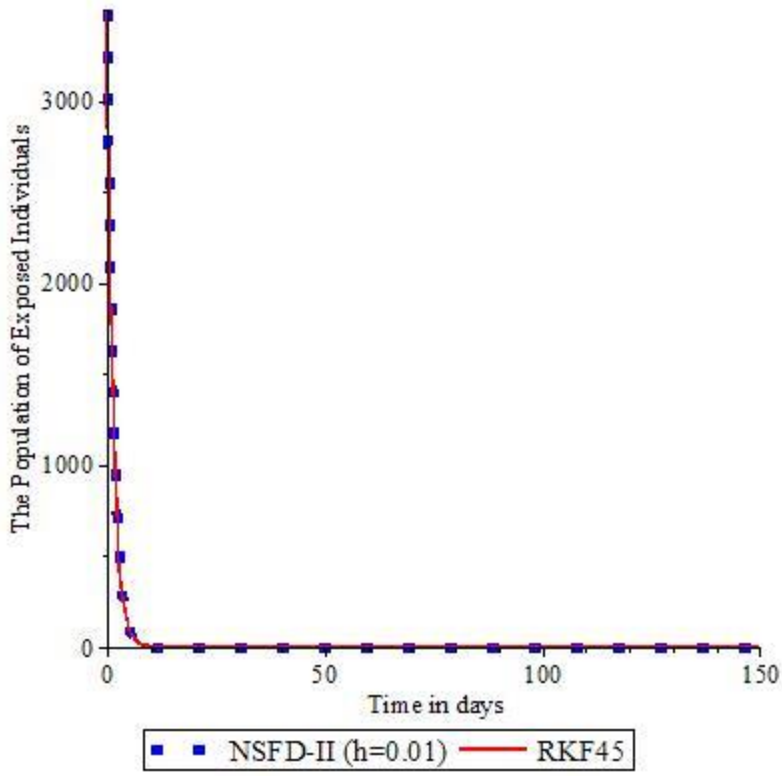

Figure 3: Graphical Comparison for $E(t)$

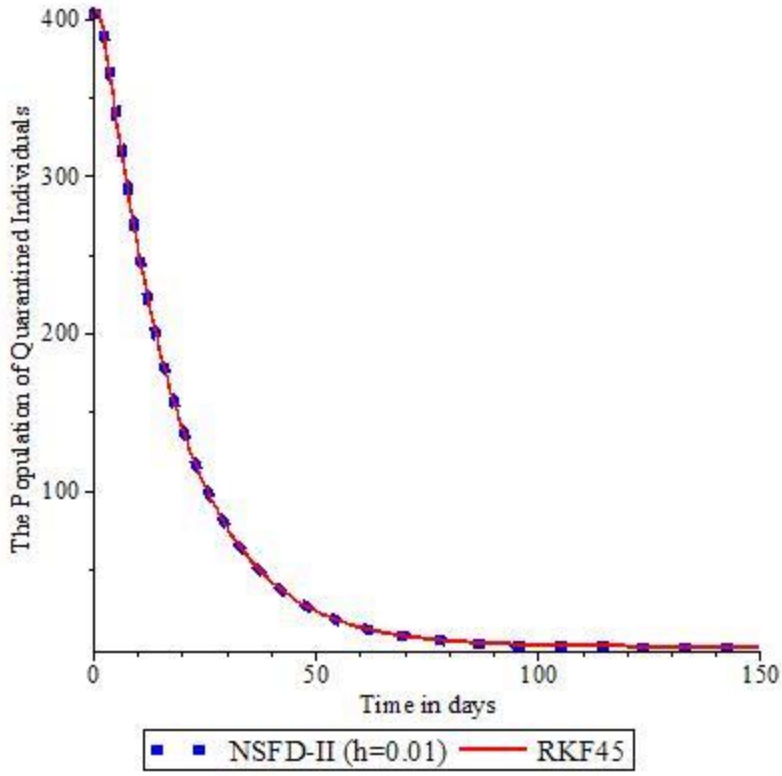

Figure 4: Graphical Comparison for $Q(t)$

Figures 5-6 present the population profile for the asymptomatic and symptomatic humans respectively. Both figures show that NSFD-II and RKF45 methods convey that the population of the individuals in the A and I compartments gradually increases first before declining to zero.

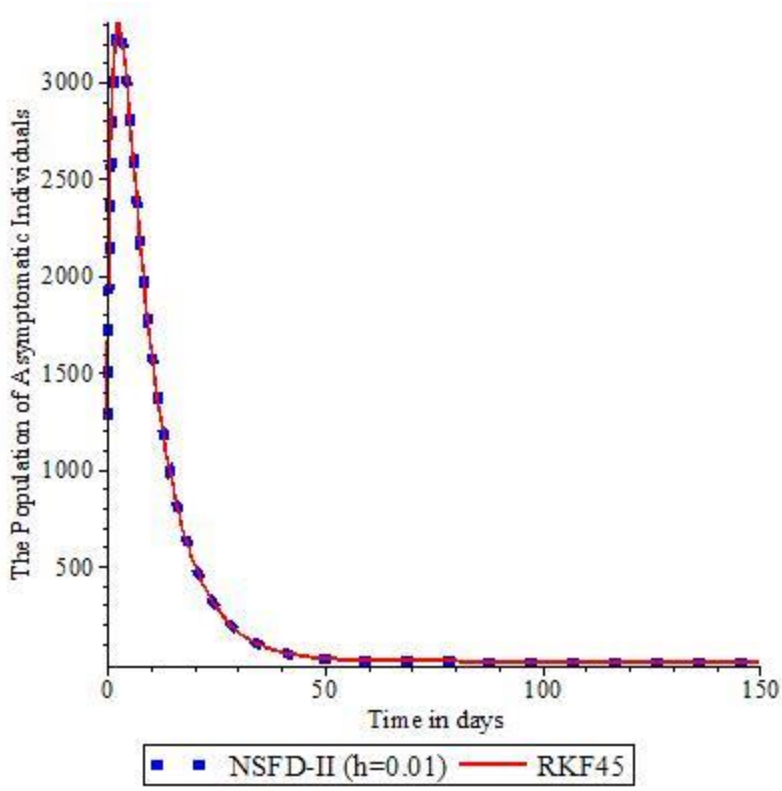

Figure 5: Graphical Comparison for $A(t)$

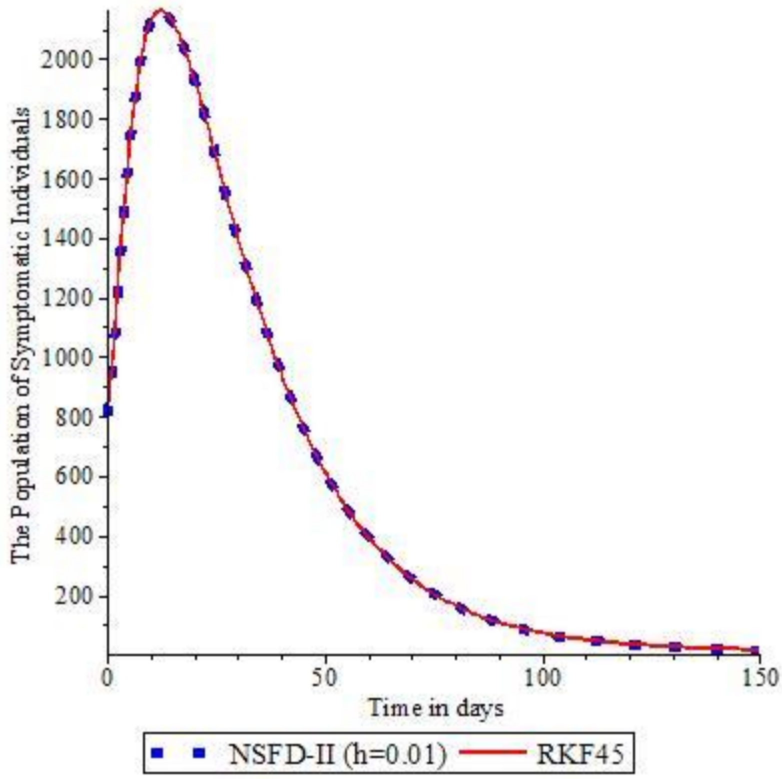

Figure 6: Graphical Comparison for $I(t)$

A graphical comparison between the results obtained by NSFD-II and RKF45 for the population of hospitalized humans is displayed in Figure 7. It is observed from Figure 7 that first there was a drop in the number of hospitalized humans, shortly followed by an increase before decreasing to zero.

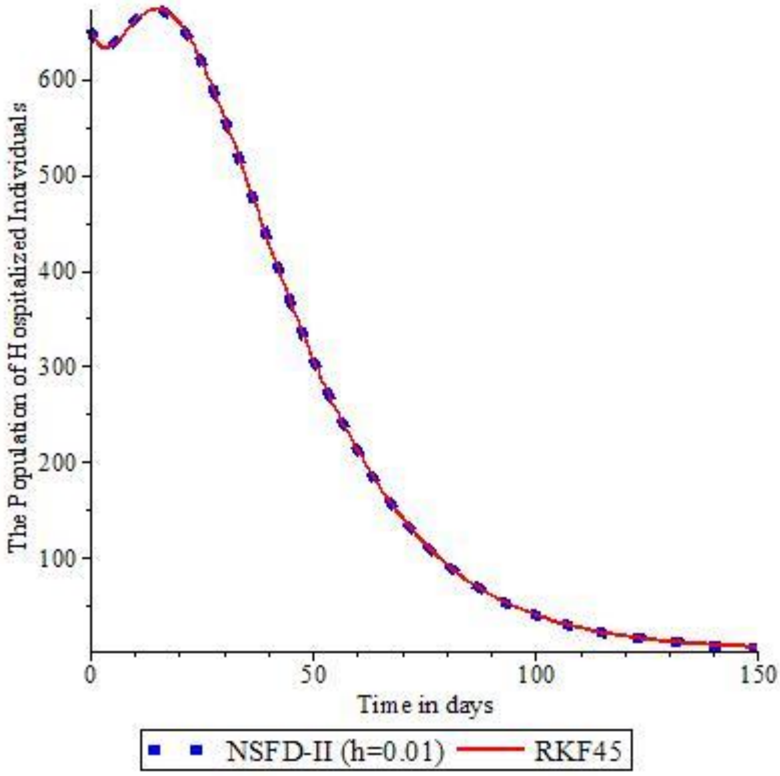

Figure 7: Graphical Comparison for $H(t)$

The population profile for the recovered individuals generated by NSFD-II and RKF45 is shown in Figure 8. The figure shows that the number of those who recovered from COVID-19 infection increases for about 60 days and later begins to decrease.

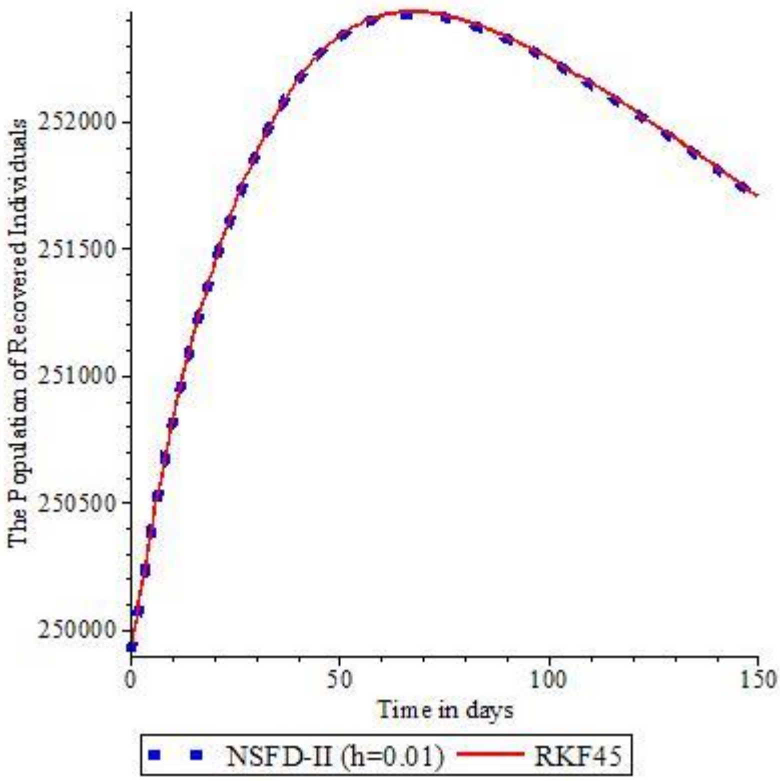

Figure 8: Graphical Comparison for $R(t)$

The population and concentration profiles for COVID-19 deceased individuals and COVID-19 viruses in the environment are depicted in Figures 9 -10 respectively. Figures 9 -10 show that $D(t)$ and $W(t)$ decreases to zero.

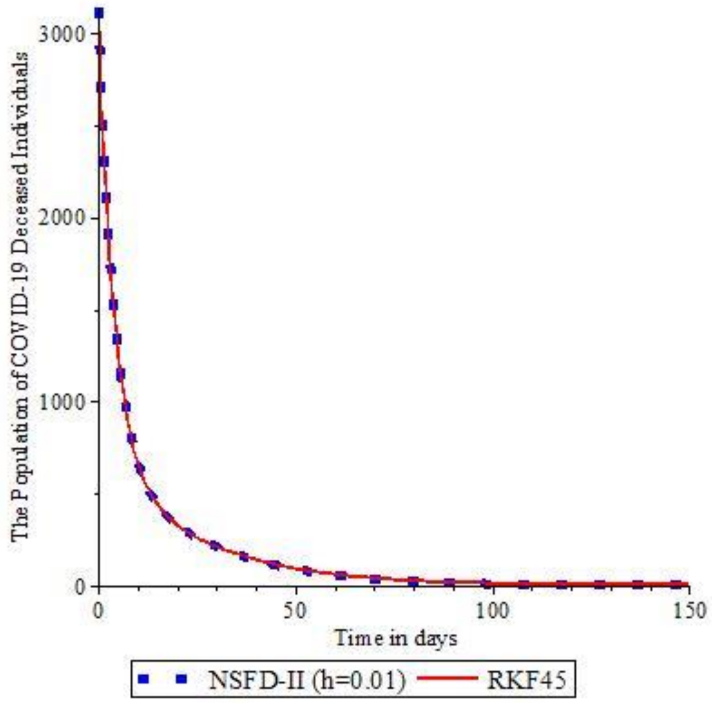

Figure 9: Graphical Comparison for $D(t)$

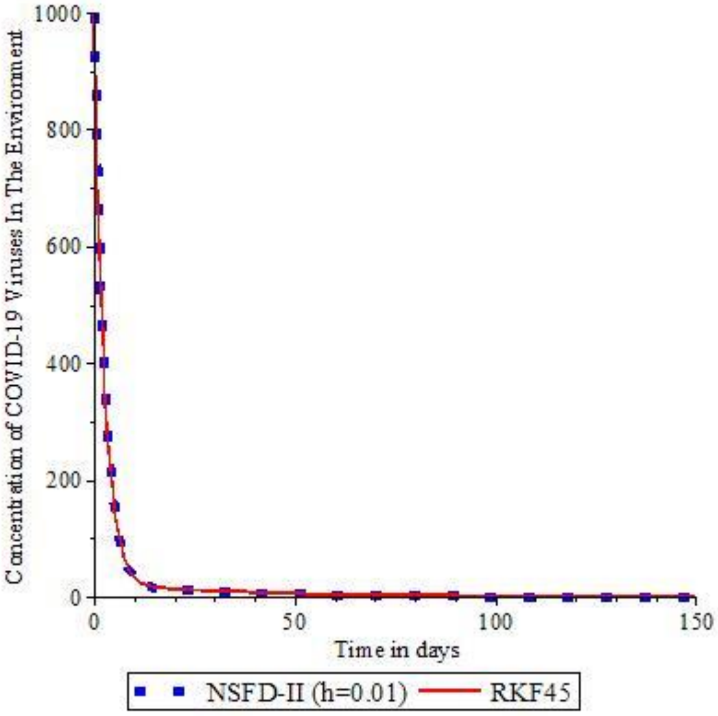

Figure 10: Graphical Comparison for $W(t)$

Finally, Figures 1-10 show that the result obtained by NSFD-II agrees excellently well with those of RKF45 despite that the default RKF45 built-in Maple 18 software makes use of adaptive step size to ensure that the absolute and relative errors for each iteration are not above $1e-7$ and $1e-6$. Thus, this makes RKF45 more cumbersome and difficult to implement when compared with NSFD-II.

CONCLUSION

An application of NSFD-II to solve a deterministic mathematical model for the transmission dynamics of COVID-19 in the presence of fear of infection was considered in this study. This model was shown to possess a unique solution that is positive and bounded. The solution obtained by NSFD-II was compared graphically with those obtained by the default Runge-Kutta Fehlberg (RKF45) built-in Maple 18 software. The comparison shows that both methods are in excellent agreement even though the RKF45 is more cumbersome and not easy to implement when compared with NSFD-II. Thus, the use NSFD-II method is reliable and efficient and should be applied to solve other nonlinear real phenomena.

REFERENCES

Aba Oud, M. A., Ali, A., Alrabaiah, H., Ullah, S., Khan, M. A., & Islam, S.(2021). A fractional order mathematical model for COVID-19 dynamics with quarantine, isolation, and environmental viral load. *Advances in Difference Equations*, 2021**(1)**: 1-19.

Adewole, M. O., Onifade, A. A., Abdullah, F. A., Kasali, F., & Ismail, A. I.(2021). Modelling the Dynamics of COVID-19 in Nigeria. *International journal of applied and computational mathematics*, 7(3):1-25.

Ahmed, H. A. O. (2011). Construction and analysis of efficient numerical methods to solve mathematical models of TB and HIV co-infection (Doctoral dissertation, University of the Western Cape).

Akinyemi, S. T., Oyelowo, Yemisi., Ibrahim, M. O. & Adamu, B. (2023). Approximate Solution of a Fractional-Order Ebola Virus Disease Model with Contact Tracing and Quarantine. *Applied Mathematics and Computational Intelligence (AMCI),* ***12***(1), 30–42.

Ashgi, R., Pratama, M. A. A., & Purwani, S. (2021). Comparison of Numerical Simulation of Epidemiological Model between Euler Method with 4th Order Runge Kutta Method. *International Journal of Global Operations Research*, 2(1): 37-44.

Butt, A. I. K., Rafiq, M., Ahmad, W., & Ahmad, N. (2023). Implementation of computationally efficient numerical approach to analyze a Covid-19 pandemic model**.** Alexandria Engineering Journal**,** 69:341-362.

Costa, G. M. R., Lobosco, M., Ehrhardt, M., & Reis, R. F. (2023). Mathematical Analysis and a Nonstandard Scheme for a Model of the Immune Response against COVID-19.1-21. Available at *https : //www.imacm.uni - wuppertal.de/fileadmin/imacm/preprints/*2023*/imacm*2302*.pdf*

Cui,Q., Xu, J., Zhang, Q. and Wang, K.(2014).An NSFD scheme for SIR epidemic models of childhood diseases with constant vaccination strategy. Advances *in Difference Equations*, 2014(172):1-15.

Derrick, W. R. and Grossman, S. I. (1987). A first course in differential equations with applications. West Publishing Company.

Diagne, M. L., Rwezaura, H., Tchoumi, S. Y., & Tchuenche, J. M. (2021). A mathematical model of COVID-19 with vaccination and treatment. *Computational and Mathematical Methods in Medicine*, 2021:1-16.

Dietz, K., & Heesterbeek, J. A. P. (2002). Daniel Bernoulli's epidemiological model revisited. *Mathematical Biosciences*, 180(2): 1-21.

Egbelowo, O. (2018). Nonlinear elimination of drugs in one-compartment pharmacokinetic models: nonstandard finite difference approach for various routes of administration. Mathematical and Computational Applications**,** 23(2):1-21.

Egbelowo, O. F., & Hoang, M. T. (2021). Global dynamics of target-mediated drug disposition models and their solutions by nonstandard finite difference method. *Journal of Applied Mathematics and Computing*, 66: 621-643.

Elaiw, A. M., Aljahdali, A. K., & Hobiny, A. D. (2023). Dynamical Properties of Discrete-Time HTLV-I and HIV-1 within-Host Coinfection Model. Axioms, 12(2):1-26.

Foppa, I. M. (2017). A Historical Introduction to Mathematical Modeling of Infectious Diseases: Seminal Papers in Epidemiology. Academic Press, Amsterdam.

Garba, S. M., Lubuma, J. M and Tsanou, B. (2020). Modeling the transmission dynamics of the COVID-19 Pandemic in South Africa. *Mathematical Bioscience*, 328(2):1-16

Gu, Y., Khan, M., Zarin, R., Khan, A., Yusuf, A., & Humphries, U. W. (2023). Mathematical analysis of a new nonlinear dengue epidemic model via deterministic and fractional approach. *Alexandria Engineering Journal*, 67:1-21.

Ibrahim (2022). Application of Optimal Control Theory on a Covid-19 Mathematical Model. Seminar presented at the University of Usmanu Danfodio University

Kambali, P. N., Abbasi, A., & Nataraj, C. (2023). Nonlinear dynamic epidemiological analysis of effects of vaccination and dynamic transmission on COVID-19. *Nonlinear Dynamics*, 111(1): 951-963.

Mehdizadeh K, M., Rashidi, M. M., Shokri, A., Ramos, H., & Khakzad, P. (2022). A Nonstandard Finite Difference Method for a Generalized Black-Scholes Equation. Symmetry, 14(1):1-13.

Mehdizadeh K, M., Shokri, A., Wang, Y., Bazm, S., Navidifar, G., & Khakzad, P. (2023). Qualitatively Stable Schemes for the Black-Scholes Equation. Fractal and Fractional, 7(2):1-14

Mickens, R.E. and Washington, T. (2012). A note on an NSFD scheme for a mathematical model of respiratory virus transmission. *J. Differ. Equ. Appl,* 8: 525-529.

Miller, J. J., & O'Riordan, E. (2020). Robust numerical method for a singularly perturbed problem arising in the modelling of enzyme kinetics. Biomath, 9(2):1-12.

Mohammed, S. J., & Mohammed, M. A. (2021, May). Runge-kutta numerical method for solving nonlinear influenza model. *In Journal of Physics:Conference Series*, 1879(2):1-15.

Nana-Kyere, S., Boateng, F. A., Jonathan, P., Donkor, A., Hoggar, G. K.,Titus, B. D., & Adu, I. K. (2022). Global Analysis and Optimal Control Model of COVID-19. Computational and Mathematical Methods in Medicine, 2022:1-20.

Ochi, P. O., Agada, A. A., Timothy, J., Urum, T. G., Ochi, H. T., & Nworah, D. A. (2023). Stability Analysis Of A Shigella Infection Epidemic Model At Endemic Equilibrium. *Fudma Journal of Sciences*, ***7***(3), 48-64.

Onwubuoya, C., Nwanze, D. E., Erejuwa, J. S., & Akinyemi, S. T. (2018). An Approximate Solution of a Computer Virus Model with Antivirus using Modifed Differential Transform

Method. *International Journal of Engineering Research & Technology,* 7(4): 154-161.

Onwubuoya, C., Akinyemi, S. T., Odabi, O. I., & Odachi, G. N. (2018). Numerical simulation of a computer virus transmission model using euler predictor corrector method. *IDOSR Journal of Applied Sciences*, 3(1):16-28.

Paul, A. K., & Kuddus, M. A. (2022). Mathematical analysis of a COVID-19 model with double dose vaccination in Bangladesh. *Results in Physics,* 35:1-13.

Peter, O. J., Shaikh, A. S., Ibrahim, M. O., Nisar, K. S., Baleanu, D., Khan, I., &Abioye, A. I. (2020). Analysis and dynamics of fractional order mathematical model of COVID-19 in Nigeria using atangana-baleanu operator. *Computers, Materials and Continua*, 66(2):1-10.

Rabiu, M. and Akinyemi, S.T. (2016). Global Analysis of Dengue Fever in a Variable Population.. *Journal of the Nigerian Association of Mathematical Physics***,** ***33****:363-376.*

Raza, A., Chu, Y. M., Bajuri, M. Y., Ahmadian, A., Ahmed, N., Rafiq, M., & Salahshour, S. (2022). Dynamical and nonstandard computational analysis of heroin epidemic model. *Results in Physics,* 34:1-12

Riyapan, P., Shuaib, S. E., Intarasit, A., & Chuarkham, K. (2021). Applications of the Differential Transformation Method and Multi-Step Differential Transformation Method to Solve a Rotavirus Epidemic Model.Mathematics and Statistics**,** 9(1):71-80.

Srivastav, A. K., Tiwari, P. K., Srivastava, P. K., Ghosh, M., & Kang, Y. (2021). A mathematical model for the impacts of face mask, hospitalization and quarantine on the dynamics of COVID-19 in India: deterministicvs. stochastic. *Mathematical Biosciences and Engineering*, 18(1): 182-213.

Sweilam, N. H., Soliman, I. A., & Al-Mekhlafi, S. M. (2017). Nonstandard finite difference method for solving the multi-strain TB model. *Journal of the Egyptian Mathematical Society*, **25**(2): 129-138.

ur Rehman, M. A., Kazim, M., Ahmed, N., Raza, A., Rafiq, M., Akg¨ *u*l, A.,... & Zakarya, M. (2023). Positivity preserving numerical method for epidemic model of hepatitis B disease dynamic with delay factor. *Alexandria Engineering Journal*, **64**: 505-515,

WHO. (2021a). WHO lists two additional COVID-19 vaccines for emergencyuse and COVAX roll-out: AstraZeneca/Oxford-developed vaccines to reach countries in the coming weeks . https://www.who.int/news/item/15-02-2021-who-lists-two- additional-covid-19-vaccines-for emergency-use-and-covaxroll-out (Accessed 28th July, 2021).

Worldometer. (2022). https://www.worldometers.info/world-population/nigeriapopulation. (Accessed online on the 4th of May, 2022).

Zafar, Z. U. A., Inc, M., Tchier, F., & Akinyemi, L. (2023). Stochastic suicide substrate reaction model. Physica A: Statistical Mechanics and its Applications 610**:** 1-20.